Electronic Supplementary Material (ESI) for Nanoscale.

Supporting Information for

Ligand Accommodation Causes the Anti-centrosymmetric Structure of $Au_{13}Cu_4$ Clusters with Near-Infrared Eission

Rajini Anumula,[a] Arthur Reber,[b] Pan An,[a] Chaonan Cui,[a] Mengdi Guo,[a] Haiming Wu,[a] Zhixun Luo,*[a] and Shiv. N. Khanna*[b]

[a] *Beijing National Laboratory for Molecular Sciences (BNLMS) and State Key Laboratory for Structural Chemistry of Unstable and Stable Species, and Key Laboratory of Photochemistry, Institute of Chemistry, Chinese Academy of Sciences, Beijing 100190, P.R. China.*

[b] *Department of Physics, Virginia Commonwealth University, Richmond, Virginia 23284, United States*

** Correspondence. Email: zxluo@iccas.ac.cn (Z.L.); snkhanna@vcu.edu* (S.N.K.)

Single Crystal data.

Crystal Data for $Au_{13}Cu_2N_6P_6S_6$(M =3100.38 g/mol): Black block crystal, 0.534 × 0.324 × 0.145, orthorhombic, space group $Pmc2_1$ (no. 26), a = 33.2427(8) Å, b = 17.2881(3) Å, c = 26.7466(5) Å, α = 90 °, β = 90 °, γ = 90°, V = 15371.4(5) Å^3, Z = 4, T = 110.00(10) K, μ(MoKα) = 12.784 mm^{-1}, $Dcalc$ = 1.340 g/cm^3, 170163 reflections measured (6.844° ≤ 2Θ ≤ 61.536°), 39951 unique (R_{int} = 0.1868, R_{sigma} = 0.1681) which were used in all calculations. The final R_1 was 0.1297 (I > 2σ(I)) and wR_2 was 0.3419 (all data).

Crystal Data for $C_{112}H_{92}Au_{13}Cu_4N_8P_4S_8Cl_4$($M$ =4745.02 g/mol): Black block crystal, 0.233 × 0.178 × 0.156 mm, monoclinic, space group $P2_1/n$ (no. 14), a = 15.5758(4) Å, b = 44.4218(10) Å, c = 41.4738(13) Å, α = 90 °, β = 95.249(2) °, γ = 90°, V = 28575.6(13) Å^3, Z = 8, T = 170.00(10) K, μ(MoKα) = 14.071 mm^{-1}, $Dcalc$ = 2.206 g/cm^3, 269977 reflections measured (6.736° ≤ 2Θ ≤ 50.4°), 51251 unique (R_{int} = 0.1470, R_{sigma} = 0.1187) which were used in all calculations. The final R_1 was 0.1144 (I> 2σ(I)) and wR_2 was 0.2305 (all data).

Single Crystal Analysis of $Au_{13}Cu_2$, $Au_{13}Cu_4$: The diffraction data of$Au_{13}Cu_2$, $Au_{13}Cu_4$ were collected on an XtaLAB AFC10 (RCD3) fixed-chi single crystal diffractometer using Mo Kα (λ = 0.71069Å). The crystal was kept at 103.00(10) K during data collection. Using Olex2 [1], the structure was solved with the SHELXT [2] structure solution program using Intrinsic Phasing and refined with the SHELXL [3] refinement package using Least Squares minimization.

Table S1: Crystallographic data for compounds $Au_{13}Cu_4$ and $Au_{13}Cu_2$ NCs.

	$Au_{13}Cu_2$	**$Au_{13}Cu_4$**
Empirical formula	$Au_{13}Cu_2N_2S_{12}$	$C_{112}H_{92}Au_{13}Cu_4N_8P_4S_8$
Formula weight	3100.38	4745.02
Crystal system, space group	Orthorhombic, $Pmc2_1$	monoclinic, $P2_1/n$
a, Å	33.2427(8)	15.5758(4)
b, Å	17.2881(3)	44.4218(10)
c, Å	26.7466(5)	41.4738(13)
α, deg.	90	90
β, deg	90	95.249(2)
γ, deg	90	90
Volume, Å3	15371.4(5)	28575.6(13)
Z	4	8
ρ calcd, g·cm-3	1.340	2.206
μ, mm-1	12.784	14.071
Temperature, K	110.00(10)	170.00(10)
θmax, deg. / Completeness, %	6.844 to 61.536	6.736 to 50.4
Reflections collected / unique	170163 / 39951 [R_{int} = 0.1868, R_{sigma} = 0.1681]	269977 / 51251 [R_{int} = 0.1470, R_{sigma} = 0.1187]
restraints / parameters	39951/1/217	51251/1587/2683
$R1^a$, $wR2^b$ [$I > 2\sigma(I)$]	$R_1 = 0.1297$, $wR_2 = 0.3151$	$R_1 = 0.1144$, $wR_2 = 0.2117$
$R1^a$, $wR2^b$ (all data)	$R_1 = 0.2186$, $wR_2 = 0.3419$	$R_1 = 0.1644$, $wR_2 = 0.2305$

Goodness of fit	1.644	1.644
Largest diff. peak and hole, e/Å 3	11.03/-6.92	5.35/-3.96

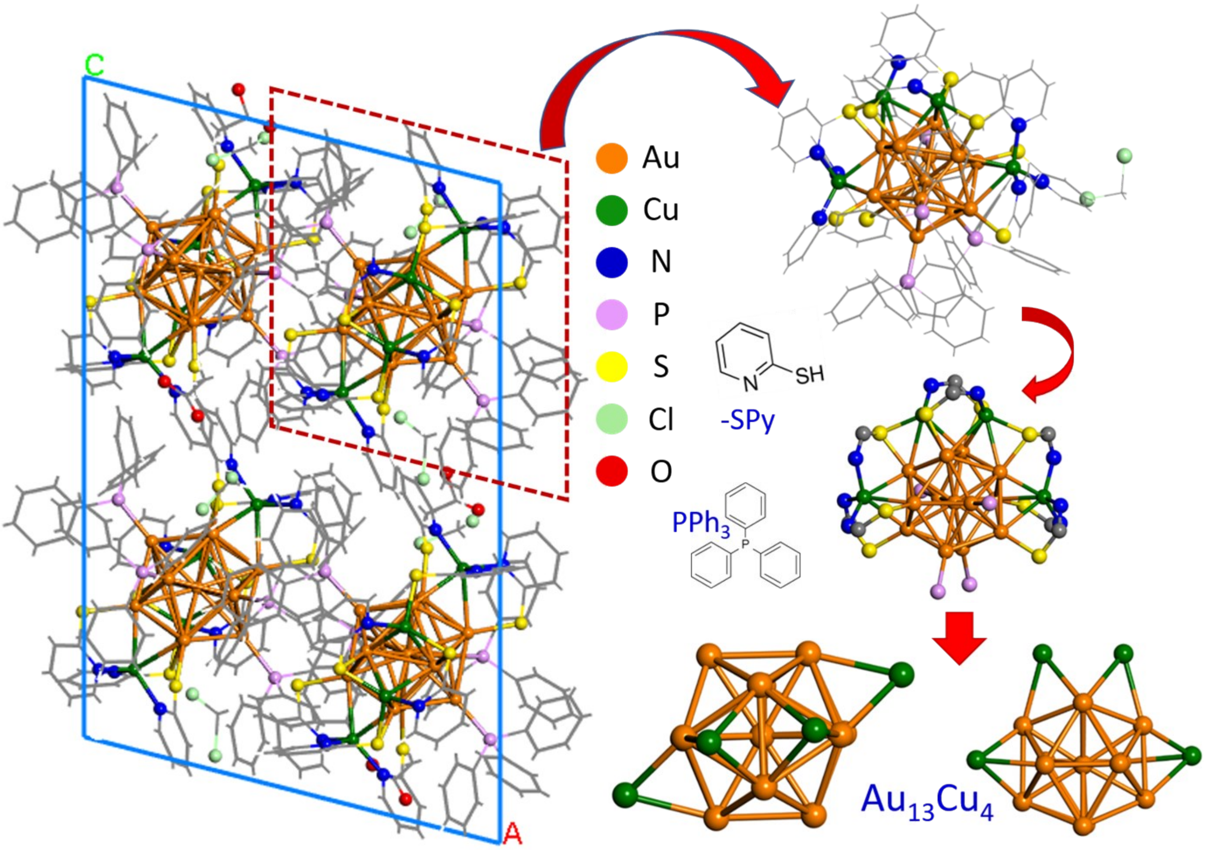

Fig. S1 Single crystal parsing of the $[Au_{13}Cu_4(PPh_3)_4(SPy)_8]^+$ cluster.

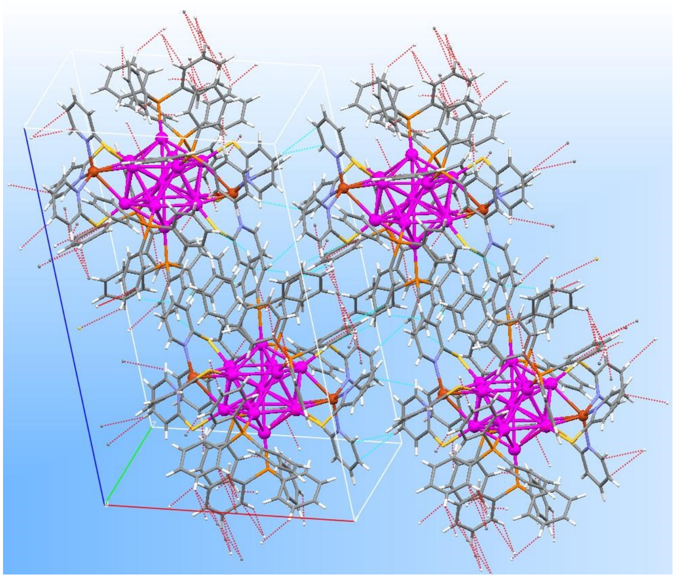

Fig. S2 Single crystal structure and stacking of the $[Au_{13}Cu_2(PPh_3)_6(SPy)_6]^+$ clusters.

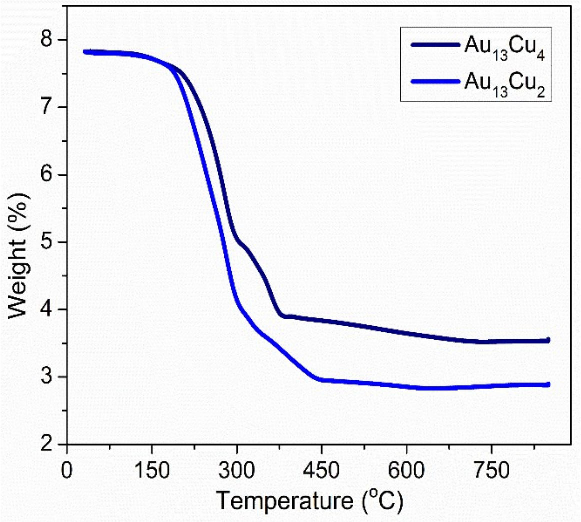

Fig. S3 TG-DTA curves of $[Au_{13}Cu_4(PPh_3)_4(SPy)_8]^+$ and $[Au_{13}Cu_2(PPh_3)_6(SPy)_6]^+$ clusters.

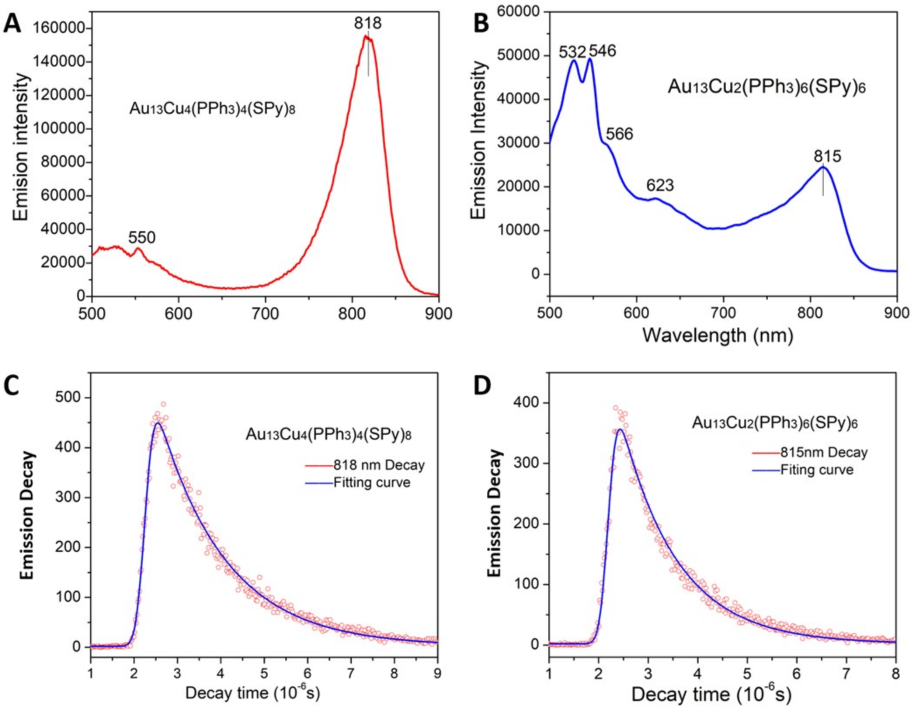

Fig. S4 (A/B) Photoluminescence spectra of the $[Au_{13}Cu_4(PPh_3)_4(SPy)_8]^+$ and $[Au_{13}Cu_2(PPh_3)_6(SPy)_6]^+$ clusters, respectively, using a 475nm excitation, measured by a normal Horiba Scientific Fluoromax-4 spectrofluorometer, as well as the time-resolved fluorescence decay **(C/D)** on a spectra physics Millenia-eV with Tsunami laser, in DCM solvent.

Time-resolved fluorescence decay measurements were carried out for the $Au_{13}Cu_2$ and $Au_{13}Cu_4$ NCs, as shown in Fig. S4 (ESI). The results on the lifetime data showed that the $Au_{13}Cu_{2,4}$ clusters exhibit long lifetime up to microseconds, specifically, 1.1 μs for $Au_{13}Cu_2$ and 1.6 μs for $Au_{13}Cu_4$ NCs. In small organic molecules, such long lifetime is often assigned to phosphorescence pertaining to $T_1 \rightarrow S_0$ transition. However, for such NCs with multi-core metal center and varied ligand-to-metal charge-transfer interactions, the mechanism could be more complex and even against the Kasha's rule.[1-6] Actually, the observation of emissions at longer wavelength range (965 and 1006 nm for $Au_{13}Cu_2$ and $Au_{13}Cu_4$ respectively) excludes the possibility of 818/815 nm peak to be assigned as phosphorescent emission as small organic molecules. The long-lifetime emissions could be normal for alloy metal NCs due to their flexible structural relaxation, multiple metal-metal and metal-ligand interactions, and hence largely increased density of states.

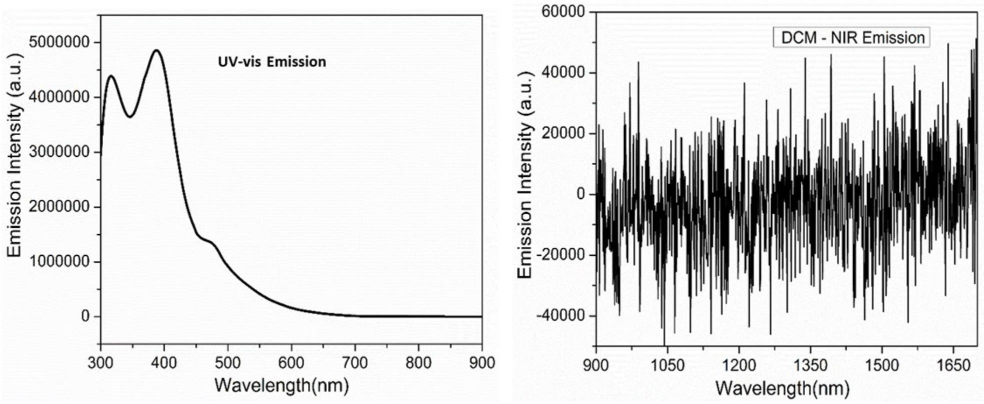

Fig. S5 Emission spectra of dichloromethane (DCM) solvent excited at 490 and 270 nm.

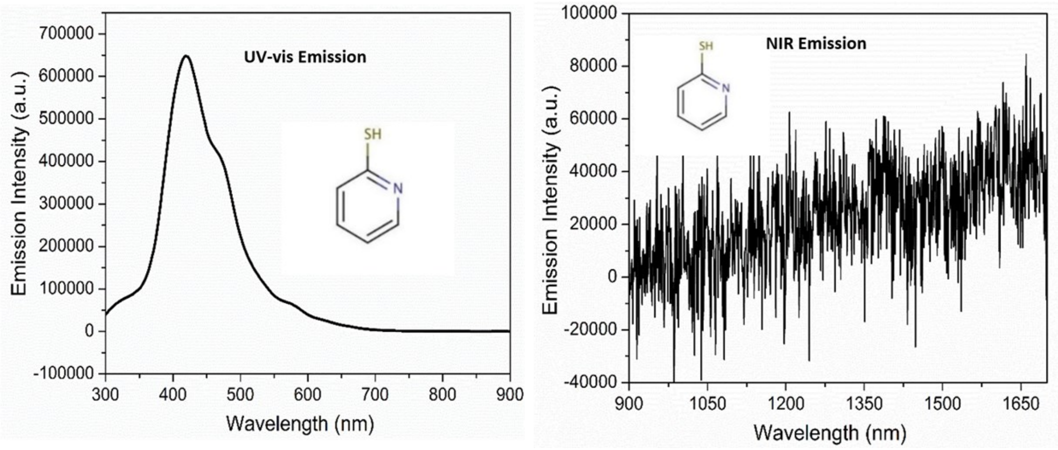

Fig. S6 Emission spectra of 2-mercaptopyrdine in DCM excited at 490 and 270 nm.

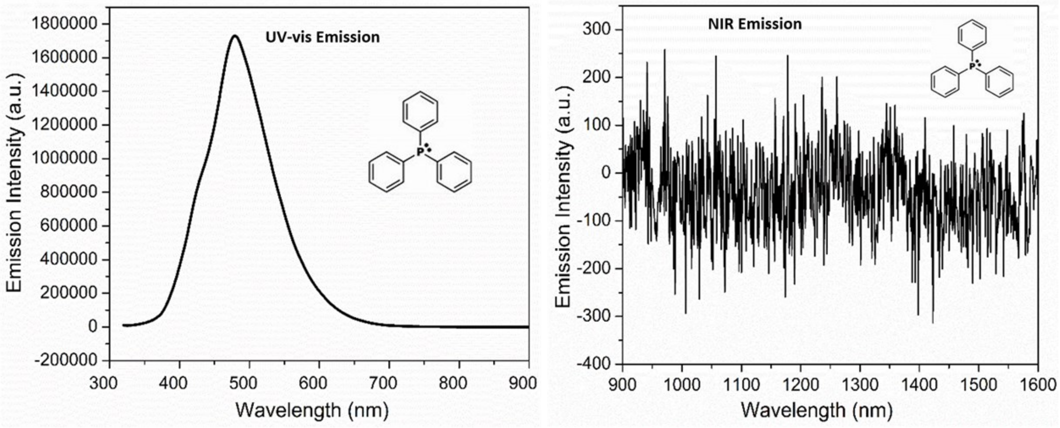

Fig. S7 Emission spectra of triphenylphosphine in DCM excited at 490 and 270 nm.

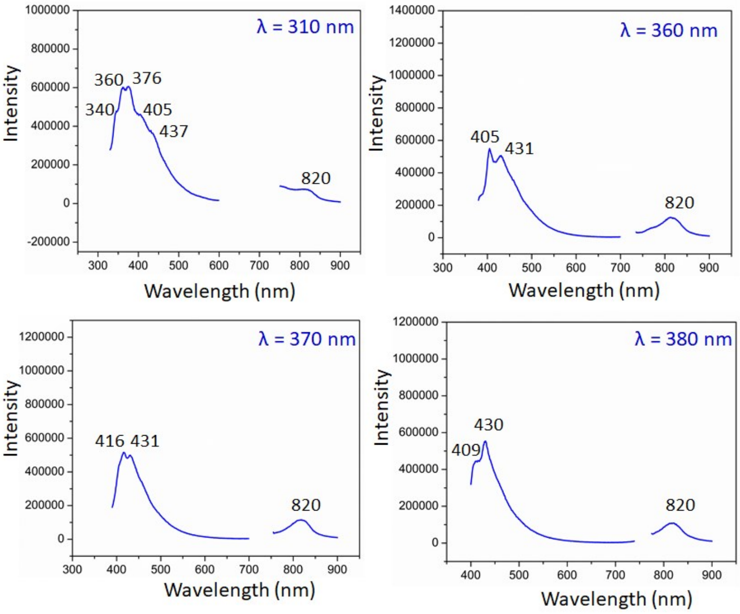

Fig. S8 Emission spectra of $[Au_{13}Cu_4(PPh_3)_4(SPy)_8]^+$ clusters excited at different wave lengths.

The excitation spectrum of $Au_{13}Cu_4$ NCs was shown in Fig. S9. The excitation spectrum was monitored with 820 nm emission wavelength produces excitation peaks at 340, 365, 465 and 475 nm, well agreement with absorption bands, indeed both the excitation and absorption spectra profiles are found to be well consistent with each other.

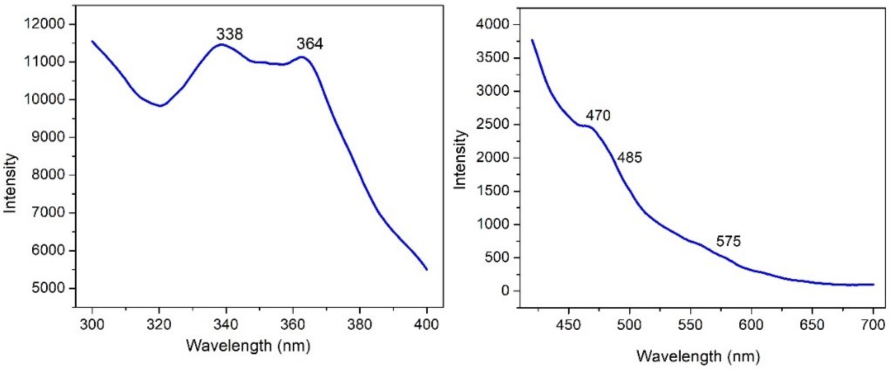

Fig. S9 Excitation spectra of $[Au_{13}Cu_4(PPh_3)_4(SPy)_8]^+$ clusters, monitored at 820nm.

References

1. Y. Zhou, G. Baryshnikov, X. Li, M. Zhu, H. Ågren and L. Zhu, *Chem. Mater.*, 2018, **30**, 8008-8016.
2. H. W. Tseng, J. Y. Shen, T. Y. Kuo, T. S. Tu, Y. A. Chen, A. P. Demchenko and P. T. Chou, *Chem Sci*, 2016, **7**, 655-665.
3. X. Qiao, Y. Liu, J. Yao, X. He, H. Liu, P. Lu and D. Ma, *J. Phys. Chem. C*, 2019, **123**, 5761-5766.
4. G. Brancato, G. Signore, P. Neyroz, D. Polli, G. Cerullo, G. Abbandonato, L. Nucara, V. Barone, F. Beltram and R. Bizzarri, *J. Phys. Chem. B*, 2015, **119**, 6144-6154.
5. A. P. Demchenko, V. I. Tomin and P. T. Chou, *Chem. Rev.*, 2017, **117**, 13353-13381.
6. R. Anumula, P. Xiao, C. Cui, H. Wu, G. Cui, W.-h. Fang, Z. Luo and J. Yao, *Nanoscale*, 2020, **12**, 7864-7869.